



Title	A new generalized particle approach to parallel bandwidth allocation
Author(s)	Feng, X; Lau, FCM; Shuai, D
Citation	Computer Communications, 2006, v. 29 n. 18, p. 3933-3945
Issued Date	2006
URL	http://hdl.handle.net/10722/53598
Rights	Creative Commons: Attribution 3.0 Hong Kong License

A New Generalized Particle Approach to Parallel Bandwidth Allocation

Xiang Feng ^a, Francis C.M. Lau ^a, Dianxun Shuai ^{b *}

^a Department of Computer Science, The University of Hong Kong, Hong Kong

^b Department of Computer Science and Engineering, East China University of Science and Technology, Shanghai, 200237, P.R. China

Abstract This paper presents a new *generalized particle* (GP) approach to dynamical optimization of network bandwidth allocation, which can also be used to optimize other resource assignments in networks. By using the GP model, the complicated network bandwidth allocation problem is transformed into the kinematics and dynamics of numerous particles in two reciprocal dual force-fields. The proposed model and algorithm are featured by the powerful processing ability under a complex environment that involves the various interactions among network entities, the market mechanism between the demands and service, and other phenomena common in networks, such as congestion, metabolism, and breakdown of network entities. The GP approach also has the advantages in terms of the higher parallelism, lower computation complexities, and the easiness for hardware implementation. The properties of the approach, including the correctness, convergency and stability, are discussed in details. Simulation results attest to the effectiveness and suitability of the proposed approach.

Keywords bandwidth allocation, generalized particle (GP), distributed parallel algorithm, computer networks, dynamical process

1 Introduction

1.1 Related work

Well-known approaches to network resource allocation include: (1) Lagrangian multiplier approaches including Kelly's[1-3] and low et al.'s[4-7]; (2) ant colony optimization approaches[8,9]; (3) max-min fairness and progressive filling algorithm[10].

The Max-Min fairness algorithm has been widely used in digital networks. It allots the bandwidths

*Corresponding author: Xiang Feng. Address: Department of Computer Science, The University of Hong Kong, Chow Yei Ching Building, Pokfulam Road, Hong Kong. Email: xfeng@cs.hku.hk.

as equally as possible to all the users under the existent transmission conditions. Although the Max-Min algorithm is easy to realize, it always gives rise to a lower availability of network bandwidth resources. Recently, algorithms based on a utility function were proposed to optimize the flow control in networks. The flow control algorithms proposed by Kelly and low et al. manage to dynamically control the data transmission rates of source nodes in networks so that the global utility of all the source nodes may be maximized. Algorithms based on a utility function can usually acquire a comparatively higher network resources availability with a certain proportional fairness. But based on centralized flow control, they are not easy to realize.

Ant colony optimization (ACO), which uses distributed control, is a novel technique for solving hard network optimization problems. ACO is based on stochastic search procedure. Their central component is the pheromone model, which is used to probabilistically sample the search space. ACO belongs to the class of meta-heuristics, which are approximate algorithms used to obtain good enough solutions to hard combinatorial optimization problems in a reasonable amount of computation time. Notwithstanding its theoretical interest, this algorithm has unknown empirical performance and requires much computation time.

In this paper, we propose a generalized particle (GP) approach, which is based on hybrid energy functions. GP has overcome the main deficiencies and retained the advantages of the well-known approaches mentioned above, as follows:

- It is easy to realize;
- It acquires a comparatively higher network resources availability;
- It controls dispersedly.

1.2 Motivation and contribution

The aim of this paper is to explore a different approach to dynamical optimization of network bandwidth allocation. We consider factors such as competition, cooperation among network entities, congestion, metabolism, breakdown of network entities, and market mechanism between the demands and service. Based on these factors and past studies in this field, an generalized particle model(GP) for

network resource allocation is proposed. The GP model takes into account all the factors just mentioned and has a good prospect in practice because it has lower time complexity.

We have proposed the *crossbar composite spring net* (CCSN) approach in [11]. CCSN takes the *elastic net* (EN) as its simplest case but can overcome EN's main deficiencies for problem solving in multi-agent systems. A CCSN consists of numerous springs coupling agent nodes, with each spring having its own time-varying force-deformation properties to represent various social interactions among the agents. These composite springs have more flexibility than EN's uniform isotropic band.

Based on CCSN, we

1. study further the particle characteristics of nodes in spring net;
2. extend the force properties of different composite springs to different forces on particles in the GP model, and study the kinematics and dynamics properties of GP such as the evolutionary mechanism, learning and particle interactions;
3. study distributed and parallel algorithms for GP and their application in networks.

The GP approach can also overcome many limitations of the CCSN approach:

1. In a CCSN, since the types of springs representing social interactions between two agents are finite, it is possible that some types of social interactions cannot be represented by appropriate springs.
2. Even though the problem nodes in a CCSN can move, they do not have autonomous self-driving forces to embody their own autonomy and personality of entities.
3. GP improves the CCSN situation by introducing the piecewise linear functions for every node (particle) so as to obtain better performance for problem solving.
4. We prove the suitability, correctness, convergency and stability of the GP approach, whereas only the correctness of the CCSN approach has been proved.

1.3 Organization

In Section 2, the generalized particle approach is introduced. In Section 3, the model for the bandwidth allocation problem is given. The parallel computing architecture and the algorithm for GP

are highlighted in Section 4. In Section 5, we present the GP model and its many interactions. In Section 6 and 7, the evolution and the properties of GP are addressed, respectively. In Section 8, we give the simulation results. Finally, conclusions are drawn in Section 9.

2 Generalized particle approach

The GP approach takes the CCSN as its simplest case but can overcome the CCSN's many deficiencies. The GP model consists of numerous particles and forces, with each particle having its own dynamics equations to represent network entities and each force having its own time-varying properties to represent various social interactions among network entities. These particles and forces have much more flexibility than CCSN's composite springs and nodes. A particle in GP can move along a specific orbit under exertion of a composite force. GP extends the composite springs and nodes of CCSN in four ways:

1. Each particle in GP has an autonomous self-driving force, to embody its own autonomy and the personality of some network entities;
2. The dynamic state of every particle in GP is a piecewise linear function of its stimulus, to guarantee a stable equilibrium state;
3. The stimulus of a particle in GP is related to its own objective, utility and intention, to realize the multiple objective optimization;
4. There are a variety of interactive forces among particles, including unilateral forces, to embody various social interactions in networks.

GP will essentially in four ways two particle-fields, entirely different from the CCSN approach which is oriented to sequencing problems in multi-agent systems.

3 Bandwidth allocation model

In networks, a path is an end-to-end relation among nodes, and is mapped the resulting split flows between the source-destination pair. The channels are route trees representing a set of paths between pairs of nodes.

We examine how best to allocate the bandwidth of a link between competing unicast and multicast traffic. We consider the scenario with a given number of links, a given number of paths, and different bandwidths allocated by each link among the channels (source-destination(s) pairs). For this study, we make several assumptions:

1. There is knowledge in every network node about every flow through an outgoing link;
2. There is knowledge in every network node about the number of paths for flow reached via an outgoing link;
3. Each node is making the bandwidth allocation independently (a particular receiver sees the bandwidth that is the minimum bandwidth of all the bandwidth allocations on the links from the source to this receiver).

The bandwidth allocation problem among m links and p channels with a total of n paths may be described by Table 1, where the notations are explained as follows:

A_i	the i -th physical link in the network;
$T_k^{(j)}$	the k -th path of the j -th channel $T^{(j)}$;
r_i	the maximum bandwidth of link A_i ;
$d^{(j)}$	the bandwidth that channel $T^{(j)}$ requires;
$x_{ik}^{(j)}$	a logical variable, $x_{ik}^{(j)} = 1$ implying that path $T_k^{(j)}$ passes link A_i , and otherwise $x_{ik}^{(j)}$ being zero;
$a_{ik}^{(j)}$	the bandwidth that link A_i allots to path $T_k^{(j)}$;
$p_{ik}^{(j)}$	the price per unit bandwidth that path $T_k^{(j)}$ tries to pay link A_i ;
$q^{(j)}$	the maximum payoff that channel $T^{(j)}$ can afford for its $d^{(j)}$;
$a_k^{(j)}$	the valid bandwidth obtained by path $T_k^{(j)}$, and $a_k^{(j)} = \min_i \{a_{ik}^{(j)} \mid \forall x_{ik}^{(j)} = 1\}$ under the assumption that, if $x_{ik}^{(j)} = 0$, then $a_{ik}^{(j)} = 0$ and $p_{ik}^{(j)} = 0$.

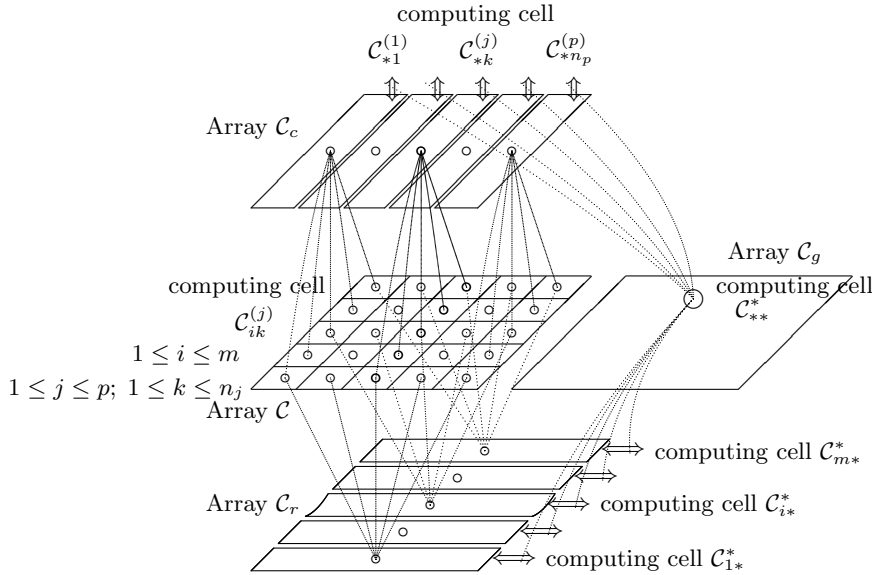
Table 1 The Bandwidth Allocation Problem.

Link \ Path	$T_1^{(1)}$...	$T_{n_1}^{(1)}$...	$T_1^{(j)}$...	$T_{n_j}^{(j)}$...	Link bandwidth
A_1	$p_{11}^{(1)}, x_{11}^{(1)}, a_{11}^{(1)}$...	$p_{1,n_1}^{(1)}, x_{1,n_1}^{(1)}, a_{1,n_1}^{(1)}$...	$p_{11}^{(j)}, x_{11}^{(j)}, a_{11}^{(j)}$...	$p_{1,n_j}^{(j)}, x_{1,n_j}^{(j)}, a_{1,n_j}^{(j)}$...	r_1
\vdots	\vdots		\vdots		\vdots		\vdots		\vdots
A_i	$p_{i1}^{(1)}, x_{i1}^{(1)}, a_{i1}^{(1)}$...	$p_{i,n_1}^{(1)}, x_{i,n_1}^{(1)}, a_{i,n_1}^{(1)}$...	$p_{i1}^{(j)}, x_{i1}^{(j)}, a_{i1}^{(j)}$...	$p_{i,n_j}^{(j)}, x_{i,n_j}^{(j)}, a_{i,n_j}^{(j)}$...	r_i
\vdots	\vdots		\vdots		\vdots		\vdots		\vdots
A_m	$p_{m1}^{(1)}, x_{m1}^{(1)}, a_{m1}^{(1)}$...	$p_{m,n_1}^{(1)}, x_{m,n_1}^{(1)}, a_{m,n_1}^{(1)}$...	$p_{m1}^{(j)}, x_{m1}^{(j)}, a_{m1}^{(j)}$...	$p_{m,n_j}^{(j)}, x_{m,n_j}^{(j)}, a_{m,n_j}^{(j)}$...	r_m
Valid bandwidth obtained by paths	$a_1^{(1)}$...	$a_{n_1}^{(1)}$...	$a_1^{(j)}$...	$a_{n_j}^{(j)}$...	
Required bandwidth and price of channels	$d^{(1)}, q^{(1)}$...	$d^{(j)}, q^{(j)}$...	

4 The parallel computing architecture and algorithm of the GP

4.1 Parallel computing architecture of the GP

A parallel implementation of GP, as shown in Fig.1, is composed of four computing cell arrays, $\mathcal{C}, \mathcal{C}_r, \mathcal{C}_c$, and \mathcal{C}_g , whose computing cells are denoted by $\mathcal{C}_{ik}^{(j)}, \mathcal{C}_{i*}^*, \mathcal{C}_{*k}^{(j)}$, and \mathcal{C}_{**}^* , respectively.



There is no interconnection between the computing cells in the same array

Fig.1 The parallel computing architecture of the GPM

The number of computing cells in each array is equal to: $n \times m$ for \mathcal{C} , n for \mathcal{C}_r , m for \mathcal{C}_c , and 1 for \mathcal{C}_g , respectively, and hence the total number of computing cells equals $n m + n + m + 1$. There is no interconnection among computing cells in the same array, whereas there are local interconnections between the following computing cell pairs: $\mathcal{C}_{*k}^{(j)}$ and \mathcal{C}_{i*}^* ; $\mathcal{C}_{ik}^{(j)}$ and $\mathcal{C}_{*k}^{(j)}$; \mathcal{C}_{i*}^* and \mathcal{C}_{**}^* ; $\mathcal{C}_{*k}^{(j)}$ and \mathcal{C}_{**}^* . It is

obvious that the connection degree of each computing cell in the array \mathcal{C} of $n \times m$ computing cells is equal to at most 2, and the unique computing cell in \mathcal{C}_g has connection degree $n+m$, with the total number of interconnections being $2nm + n + m$.

At time t in a fixed time slot ρ , the computing cell $\mathcal{C}_{ik}^{(j)}$ sends its dynamical state $q_{ik}^{(j)}(t) \langle \mathbf{a}_{ik}^{(j)}(t), \mathbf{p}_{ik}^{(j)}(t) \rangle$ to computing cells \mathcal{C}_{i*}^* and $\mathcal{C}_{*k}^{(j)}$, and receives the feedback inputs that are generated by computing cells \mathcal{C}_{i*}^* and $\mathcal{C}_{*k}^{(j)}$ at time $(t - \tau)$. By using the received $q_{ik}^{(j)}(t)$, the computing cell \mathcal{C}_{i*}^* ($\mathcal{C}_{*k}^{(j)}$, resp.) obtain its calculation state $u_{i*}^*(t)$ ($u_{*k}^{(j)}(t)$, resp.) according to equation 1 (equation 2, respectively), yielding its current output to be fed back to the computing cells $\mathcal{C}_{ik}^{(j)}$. In the meanwhile, the computing cell \mathcal{C}_{i*}^* and $\mathcal{C}_{*k}^{(j)}$ receive the feedback input from computing cell \mathcal{C}_{**}^* . The computing cell, \mathcal{C}_{i*}^* , $\mathcal{C}_{*k}^{(j)}$, and \mathcal{C}_{**}^* will change their calculation states according to equation 1, 2, 7 and 8, respectively. The computing cell $\mathcal{C}_{ik}^{(j)}$ will change its dynamical state according to equation 11 and 12, respectively.

The implementation of GP is characterized by high-degree parallelism and good scalability. All the computations of cellular dynamics both in the same array and in the different arrays are concurrently carried out. The computing cellular structure, computing cellular dynamics and the algorithm are all independent of the considered problem scale. Moreover, there is no direct interconnection among computing cells in the same array, so that it is relatively easy to implement them in VLSI technologies.

4.2 The parallel GP algorithm

Algorithm GP

Input: $r_i, d^{(j)}, q^{(j)}$

Output:

1. Initialization:

$t \leftarrow 0$

$a_{ik}^{(j)}(t), p_{ik}^{(j)}(t)$ — Initialize in parallel in $C(\mathcal{C}_{ik}^{(j)})$

2. **While** ($du_k^{(j)}(t)/dt \neq 0$ or $du_i(t)/dt \neq 0$) **do** — Judge in \mathcal{C}_g (\mathcal{C}_{**}^*)

$t \leftarrow t + 1$

$u_k^{(j)}(t)$ — Compute in parallel in C_c ($\mathcal{C}_{*k}^{(j)}$) according to Eq.(1)

$du_k^{(j)}(t)/dt$ — Compute in parallel in C_c ($\mathcal{C}_{*k}^{(j)}$) according to Eq.(7)

$u_i(t)$ — Compute in parallel in C_r (\mathcal{C}_{i*}^*) according to Eq.(2)

$du_i(t)/dt$ — Compute in parallel in C_r (\mathcal{C}_{i*}^*) according to Eq.(8)

$da_{ik}^{(j)}(t)/dt$ — Compute in parallel in $C(\mathcal{C}_{ik}^{(j)})$ according to Eq.(11)

$a_{ik}^{(j)}(t) \leftarrow a_{ik}^{(j)}(t-1) + da_{ik}^{(j)}(t)/dt$ — Compute in parallel in $C(\mathcal{C}_{ik}^{(j)})$

$dp_{ik}^{(j)}(t)/dt$ — Compute in parallel in $C(\mathcal{C}_{ik}^{(j)})$ according to Eq.(12)

$p_{ik}^{(j)}(t) \leftarrow p_{ik}^{(j)}(t-1) + dp_{ik}^{(j)}(t)/dt$ — Compute in parallel in $C(\mathcal{C}_{ik}^{(j)})$

The algorithm GP has general of complexity $\mathcal{O}(m+n)$ where $m+n$ is the number of particles. The time complexity of the algorithm is $\mathcal{O}(I_1)$, where I_1 is the number of iterations for Costep 2 (the while loop).

5 The GP model

In this model, network links and paths are treated as two kinds of generalized particles that are located in two force-fields, respectively, hence transforming the bandwidth allocation process into the kinematics and dynamics of the particles in the two force-fields.

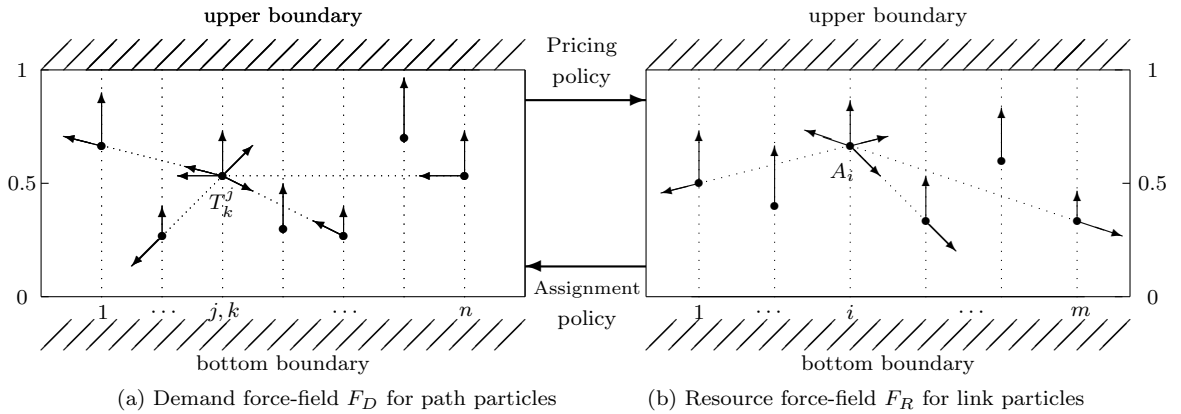


Fig.2 Generalized particle model to optimize the network bandwidth allocation.

Particle and *force-field* are two concepts of physics. Particles in this generalized particle model move not only under outside forces, but also under internal force; hence they are different from particles in physics. As shown in Fig. 2, the link particles that have bandwidth resources move in the resource force-field F_R , and the path particles that require bandwidth assignment move in the demand force-field F_D . The force fields, F_R and F_D , are geometrically independent, without any forces directly exerted from each other, but they are mutually influenced and conditioned each other through such a reciprocal procedure that the allocation policy of the link particles and the payment policy of the path particles change alternatively. In this way, the two force-fields form a reciprocal dual force field.

The vertical coordinate of a particle in force-field F_R or F_D represents the utility of the network link or path that is described by the particle. A particle will be influenced simultaneously by several kinds of forces, which include the gravitational force of the force-field where the particle is located, the pulling or pushing forces stemming from the interactions with other particles in the same force-field, and

its own autonomous driving force. In our model, all these forces are dealt with as the forces only along the vertical. Thus a particle will be driven by the resultant force of all the forces to move upwards or downwards. The larger the upward resultant force on a particle, the faster the upward movement of the particle. When the upward resultant force on a particle is equal to zero, the particle will stop moving, being at an equilibrium status.

The upward gravitational force of a force-field on a particle contributes an upward component of the motion of the particle, which represents the tendency that the particle pursues the common benefit of the whole. The upward or downward component of the motion of a particle, that is related to the interactions with other particles, depends upon the strengths and categories of the interactions. A particle's own autonomous driving force is proportional to the degree the particle tries to move upwards in the force-field where it is located, i.e. the entity (network link or path) tries to acquire its own maximum profit. The difference between the particle of the proposed generalized particle model and the particle of a classical physical model is that the generalized particle has its own driving force which depends upon the autonomy of the particle. All the generalized particles both in the same force-field and in different force-fields simultaneously evolve under their exerted forces, and, as long as they gradually reach their equilibrium positions from their initial positions, we can obtain a feasible solution to the optimization of bandwidth allocation.

As for the interactions among the link particles during the optimization of network bandwidth allocation, if two links belong to different paths, then they will compete with each other so that each of them might obtain its own maximal benefit via its own bandwidth allocation, and hence the two corresponding link particles in the force-field F_R mutually exert the forces that try to drive the other side downwards. If two links belong to the same path, then in order to obtain some benefit from the bandwidths that are assigned to the path by the two links, they have to cooperate so that their assigned bandwidths to the path are as equal as possible, and accordingly the two corresponding link particles in the force-field F_R yield the forces that attempt to push the other side upwards. Similarly, for the interactions among the path particles, if two network paths that share some common links belong to different channels, then they compete with each other for bandwidth of the shared links. Hence the two

corresponding path particles in the force-field F_D exert each other the forces that try to pull the other side downwards. If two network paths belong to the same channel, then in order to satisfy the requirement for the total bandwidth of the channel, they have to cooperate.

Meanwhile, the market mechanism may play an important role for the optimization of network bandwidth allocation. The bandwidth allocation policy of a network link and the payment policy of a network path will dynamically change according to the situation of the demands and supplies of bandwidths, which will influence the kinematics and dynamics of the link particles and path particles in their force-fields. In general, a network path always wishes to pay as little as possible under the condition that its bandwidth requirement could be satisfied, which is embodied in our model by that the corresponding path particle is usually driven upwards by the gravitational force of the force-field F_D . Similarly, to maximize its benefit a link usually tries to assign its own bandwidth to such a path that may pay the maximal price for unit bandwidth, which is embodied by the upward movement tendency of the corresponding link particle that is driven by the upward gravitational force of the force-field F_R . Moreover, in order to optimize the bandwidth allocation in the cases of intermittent congestion, normal metabolism and random breakdown occur in networks, we can make use of the congestion factor, metabolism factor, breakdown factor and priority factor in the kinematical and dynamical equations of the generalized particle model.

6 Evolution of GP

The mathematical model based on GP for dynamic bandwidth allocation that involves m links, n paths and p channels is defined as follows.

Definition 1 Let $u_k^{(j)}(t)$ be the distance from the current position of the path particle $T_k^{(j)}$ to the upper boundary of the demand force- field F_D at time t , and let $J_D(t)$ be the whole utility of all the path particles in F_D . We define $u_k^{(j)}(t)$ and $J_D(t)$, respectively, by

$$u_k^{(j)}(t) = \varsigma_1 \exp \left[- \sum_{i=1}^m a_k^{(j)}(t) / p_{ik}^{(j)}(t) \right]; \quad J_D(t) = \alpha_1 \sum_{j=1}^p \sum_{k=1}^{n_j} u_k^{(j)}(t) \quad (1)$$

Let $u_i(t)$ be the distance from the current position of the link particle A_i to the upper boundary of the resource force- field F_R at time t , and let $J_R(t)$ be the whole utility of all the link particles in F_R . We define $u_i(t)$ and $J_R(t)$, respectively, by

$$u_i(t) = \varsigma_2 \exp \left[- \sum_{j=1}^p \sum_{k=1}^{n_j} p_{ik}^{(j)}(t) / a_{ik}^{(j)}(t) \right]; \quad J_R(t) = \alpha_2 \sum_{i=1}^m u_i(t) \quad (2)$$

Where $\varsigma_1, \varsigma_2 > 1$, and $0 < \alpha_1, \alpha_2 < 1$.

Definition 2 At time t , the potential energy functions, $P_D(t)$ and $P_R(t)$, that are caused by the upward gravitational forces of the force-fields, F_D and F_R , respectively, are defined by

$$P_D(t) = \epsilon^2 \ln \sum_{j=1}^p \sum_{k=1}^{n_j} \exp[(u_k^{(j)}(t))^2 / 2\epsilon^2] - \epsilon^2 \ln n \quad (3)$$

$$P_R(t) = \epsilon^2 \ln \sum_{i=1}^m \exp[u_i^2(t) / 2\epsilon^2] - \epsilon^2 \ln m \quad (4)$$

Where $0 < \epsilon < 1$, $n = \sum_{j=1}^p n_j$, n_j is the number of the paths that belong to the j -th channel $T^{(j)}$.

Definition 3 At time t , the potential energy functions, $Q_D(t)$ and $Q_R(t)$, that are caused by the interactive forces among the particles in F_D and F_R , respectively, are defined by

$$Q_D(t) = \beta_1 \sum_{j=1}^p \left| \sum_{k=1}^{n_j} a_k^{(j)}(t) - d^{(j)}(t) \right|^2 + \rho \sum_{j=1}^p \left| \sum_{k=1}^{n_j} \sum_{i=1}^m a_{ik}^{(j)}(t) p_{ik}^{(j)}(t) - q^{(j)}(t) \right|^2 + E_D(t) \quad (5)$$

$$Q_R(t) = \beta_2 \sum_{i=1}^m \left| \sum_{j=1}^p \sum_{k=1}^{n_j} a_{ik}^{(j)}(t) - r_i(t) \right|^2 + E_R(t) \quad (6)$$

Where $0 < \beta_1, \beta_2, \rho < 1$; the first and second terms of $Q_D(t)$, and the first term of $Q_R(t)$ are all related to the constraints for bandwidth allocation; $E_D(t)$ and $E_R(t)$ are the potential energy functions that involve other kinds of the interactive forces among the particles in F_D and F_R , respectively.

$E_R(t)$ of Eq. (6) can be defined by $E_R(t) = \sum_{i,j} E(u_i, u_j)$, where $E(u_i, u_j)$ represents the potential energy function that is produced by the interactive force of the link particle A_i with respect to A_j . For two particles that compete with each other, the interactive potential energy functions are all positive. While for two particles that cooperate with each other, the interactive potential energy functions are all negative. In general, it may be that $E(u_i, u_j) \neq E(u_j, u_i)$, which implies that both the magnitudes and signs of the interactive forces between two link particles may be different. In addition to the competitive and cooperative interactions, by using the interactive potential energy we thus may describe various social coordinations among the particles, including bilateral or unilateral, and awareness or unawareness. For examples, if the link particle A_i takes an enticement or deception action on A_j , then $E(u_j, u_i) = 0$ and $E(u_i, u_j) > 0$ because the interactions between them are unilateral social coordination. Moreover, if

A_i takes an avoidance or concession action with respect to A_i , then, also due to their unilateral social coordination, we may have $E(u_j, u_i) > 0$ and $E(u_i, u_j) = 0$. If there is no interaction between them, then $E(u_i, u_j) = E(u_j, u_i) = 0$. In some cases, we may also define $E(u_i, u_j) = \pm \frac{1}{2} \mu_{ij} (u_i + u_j)^2$, which means the interactive force of A_i with respect to A_j is a linear function of the distances u_i and u_j . If the interactive force of A_i with respect to A_j is a time-varying non-linear function of the distances u_i and u_j , then we may define $E(u_i, u_j) = \pm \int_0^{u_i+u_j} (1 - \exp(-\mu_{ij}x)) dx$, where $\mu_{ij} < 0$ and $\mu_{ij} \neq \mu_{ji}$ represents the different interactive strengths of A_i with respect to A_j and of A_j with respect to A_i . Similarly, we can define $E_D(t)$ of Eq. (5) for the path particles in F_D .

Definition 4 *Dynamic equations for path particle $T_k^{(j)}$ and link particle A_i are defined, respectively, as follows.*

$$\begin{cases} du_k^{(j)}(t)/dt = \Phi_1(t) + \Phi_2(t) \\ \Phi_1(t) = -u_k^{(j)}(t) + \gamma_1 v_k^{(j)}(t) \\ \Phi_2(t) = -[\eta_1 + \eta_2 \frac{\partial J_D(t)}{\partial u_k^{(j)}(t)} + \eta_3 \frac{\partial P_D(t)}{\partial u_k^{(j)}(t)} + \eta_4 \frac{\partial Q_D(t)}{\partial u_k^{(j)}(t)}] \sum_{i=1}^m [\frac{\partial u_k^{(j)}(t)}{\partial P_{ik}^{(j)}(t)}]^2 \end{cases} \quad (7)$$

$$\begin{cases} du_i(t)/dt = \Psi_1(t) + \Psi_2(t) \\ \Psi_1(t) = -u_i(t) + \gamma_2 v_i(t) \\ \Psi_2(t) = -[\lambda_1 + \lambda_2 \frac{\partial J_R(t)}{\partial u_i(t)} + \lambda_3 \frac{\partial P_R(t)}{\partial u_i(t)} + \lambda_4 \frac{\partial Q_R(t)}{\partial u_i(t)}] \sum_{j=1}^p \sum_{k=1}^{n_j} [\frac{\partial u_i(t)}{\partial a_{ik}^{(j)}(t)}]^2 \end{cases} \quad (8)$$

$$v_k^{(j)}(t) = \begin{cases} 0 & \text{if } u_k^{(j)}(t) < 0 \\ u_k^{(j)}(t) & \text{if } 0 \leq u_k^{(j)}(t) \leq 1 \\ 1 & \text{if } u_k^{(j)}(t) > 1, \end{cases} \quad (9)$$

$$v_i(t) = \begin{cases} 0 & \text{if } u_i(t) < 0 \\ u_i(t) & \text{if } 0 \leq u_i(t) \leq 1 \\ 1 & \text{if } u_i(t) > 1, \end{cases} \quad (10)$$

Where, $v_k^{(j)}(t)$ is a piecewise linear function of $u_k^{(j)}(t)$; $v_i(t)$ is a piecewise linear function of $u_i(t)$; $\gamma_1, \gamma_2 > 1$; $0 \leq \eta_1, \eta_2, \eta_3, \eta_4, \lambda_1, \lambda_2, \lambda_3, \lambda_4 < 1$.

In order to dynamically optimize network bandwidth allocation, link particles in F_R and path particles in F_D will alternately change their own policy regarding bandwidth assignment and bandwidth

prices, respectively. On one hand, path particle $T_k^{(j)}$ modifies its price, $p_{ik}^{(j)}$, for unit bandwidth that is given by link A_i as follows:

$$dp_{ik}^{(j)}(t)/dt = -\eta_1 \frac{\partial u_k^{(j)}(t)}{\partial p_{ik}^{(j)}(t)} - \eta_2 \frac{\partial J_D(t)}{\partial p_{ik}^{(j)}(t)} - \eta_3 \frac{\partial P_D(t)}{\partial p_{ik}^{(j)}(t)} - \eta_4 \frac{\partial Q_D(t)}{\partial p_{ik}^{(j)}(t)} \quad (11)$$

On the other hand, link particle A_i updates the bandwidth $a_{ik}^{(j)}$ that is allotted to path $T_k^{(j)}$ as follows:

$$da_{ik}^{(j)}(t)/dt = -\lambda_1 \frac{\partial u_i(t)}{\partial a_{ik}^{(j)}(t)} - \lambda_2 \frac{\partial J_R(t)}{\partial a_{ik}^{(j)}(t)} - \lambda_3 \frac{\partial P_R(t)}{\partial a_{ik}^{(j)}(t)} - \lambda_4 \frac{\partial Q_R(t)}{\partial a_{ik}^{(j)}(t)} \quad (12)$$

According to the equations (1), (3), (5), we have

$$\begin{aligned} \frac{\partial u_k^{(j)}(t)}{\partial p_{ik}^{(j)}(t)} &= a_k^{(j)}(t) u_k^{(j)}(t) / [p_{ik}^{(j)}(t)]^2 ; \\ \frac{\partial J_D(t)}{\partial p_{ik}^{(j)}(t)} &= \frac{\partial J_D(t)}{\partial u_k^{(j)}(t)} \frac{\partial u_k^{(j)}(t)}{\partial p_{ik}^{(j)}(t)} = \alpha_1 a_k^{(j)}(t) u_k^{(j)}(t) / [p_{ik}^{(j)}(t)]^2 ; \\ \frac{\partial P_D(t)}{\partial p_{ik}^{(j)}(t)} &= \frac{\partial P_D(t)}{\partial u_k^{(j)}(t)} \frac{\partial u_k^{(j)}(t)}{\partial p_{ik}^{(j)}(t)} = \omega_k^{(j)}(t) a_k^{(j)}(t) [u_k^{(j)}(t) / p_{ik}^{(j)}(t)]^2 ; \\ \frac{\partial Q_D(t)}{\partial p_{ik}^{(j)}(t)} &= \rho \frac{\partial |\sum_{k=1}^{n_j} \sum_{i=1}^m a_{ik}^{(j)}(t) p_{ik}^{(j)}(t) - q^{(j)}(t)|^2}{\partial p_{ik}^{(j)}(t)} + \frac{\partial E_D(t)}{\partial u_k^{(j)}(t)} \frac{\partial u_k^{(j)}(t)}{\partial p_{ik}^{(j)}(t)} \\ &= 2\rho a_{ik}^{(j)}(t) [\sum_{k=1}^{n_j} \sum_{i=1}^m a_{ik}^{(j)}(t) p_{ik}^{(j)}(t) - q^{(j)}(t)] + a_k^{(j)}(t) u_k^{(j)}(t) \frac{\partial E_D(t)}{\partial u_k^{(j)}(t)} / [p_{ik}^{(j)}(t)]^2 ; \end{aligned}$$

where, $\omega_k^{(j)}(t) = \exp [(u_k^{(j)}(t))^2 / 2\epsilon^2] / \sum_{j=1}^p \sum_{k=1}^{n_j} \exp [(u_k^{(j)}(t))^2 / 2\epsilon^2]$. When the values of $a_k^{(j)}(t)$, $u_k^{(j)}(t)$ and $p_{ik}^{(j)}(t)$ are known at time t , substituting them into (11) gives $dp_{ik}^{(j)}(t)/dt$. Similarly, When the values of $a_{ik}^{(j)}(t)$, $u_i(t)$ and $p_{ik}^{(j)}(t)$ are given at time t , then $da_{ik}^{(j)}(t)/dt$ can be obtained by substituting the following equations into (12).

$$\begin{aligned} \frac{\partial u_i(t)}{\partial a_{ik}^{(j)}(t)} &= p_{ik}^{(j)}(t) u_i(t) / [a_{ik}^{(j)}(t)]^2 ; \quad \frac{\partial J_R(t)}{\partial a_{ik}^{(j)}(t)} = \alpha_2 p_{ik}^{(j)}(t) u_i(t) / [a_{ik}^{(j)}(t)]^2 ; \\ \frac{\partial P_R(t)}{\partial a_{ik}^{(j)}(t)} &= \omega_i(t) p_{ik}^{(j)}(t) [u_i(t) / a_{ik}^{(j)}(t)]^2 , \quad \omega_i(t) = \exp [(u_i(t))^2 / 2\epsilon^2] / \sum_{i=1}^m \exp [(u_i(t))^2 / 2\epsilon^2] ; \\ \frac{\partial Q_R(t)}{\partial a_{ik}^{(j)}(t)} &= 2\beta_2 [\sum_{j=1}^p \sum_{k=1}^{n_j} a_{ik}^{(j)}(t) - r_i(t)] + p_{ik}^{(j)}(t) u_i(t) \frac{\partial E_R(t)}{\partial u_i(t)} / [a_{ik}^{(j)}(t)]^2 . \end{aligned}$$

7 Properties of GP

In this section, we discuss the suitability, correctness, convergency and stability of the generalized particle model and algorithm. Theorem 1 through Theorem 6 elucidate the correctness of the GP algorithm. It turns out that every path particle and link particle will correctly adapt the pricing policy and allocation policy, respectively, so that the bandwidth allocation could be optimized. Furthermore, they

will correctly change their intention strength with respect to maximizing their own personal utility or the whole system utility, and correctly adjust their interactions with other particles, so that the bandwidth allocation could be realized under a very complicated environment by using the GP algorithm. Theorem 7 through Theorem 9 indicate that all the particles converge to their stable equilibrium states through the GP algorithm.

Theorem 1 *Updating the price $p_{ik}^{(j)}$ per unit bandwidth by Eq. (11) amounts to giving rise to the speed increment $\Phi_2(t)$ of Eq. (7) for the path particle $T_k^{(j)}$. Updating the allotted bandwidth $a_{ik}^{(j)}$ by Eq. (12) amounts to giving rise to the speed increment $\Psi_2(t)$ of Eq. (8) for the link particle A_i .*

Theorem 2 *The first and second terms of Eq. (11) will enable the path particle $T_k^{(j)}$ to increase its personal utility in direct proportion to the value of $(\eta_1 + \alpha_1 \eta_2)$. The first and second terms of Eq. (12) will cause the link particle A_i to increase its personal utility in direct proportion to the value of $(\lambda_1 + \alpha_2 \lambda_2)$.*

Lemma 1 *For the generalized particle model and algorithm GP, if ϵ is very small, then decreasing the potential energy $P_R(t)$ of Eq. (4) for the resource force-field $F_R(t)$ amounts to increasing the utility of such a link whose utility is minimal among all the links. If ϵ is very small, then decreasing the potential energy $P_D(t)$ of Eq. (4) for the demand force-field $F_D(t)$ amounts to increasing the utility of such a path whose utility is minimal among all the paths.*

Theorem 3 *For the generalized particle model and algorithm GP, updating the price $p_{ik}^{(j)}$ for unit bandwidth according to Eq. (11) amounts to increasing the minimal utility among all the path particles in direct proportion to the value of $\eta_3 [\omega_k^{(j)}(t)]^2$. Updating the allotted bandwidth $a_{ik}^{(j)}$ according to Eq. (12) amounts to increasing the minimal utility among all the link particles in direct proportion to the value of $\lambda_3 \omega_i^2(t)$.*

Theorem 4 For the generalized particle model and algorithm GP, when a path particle $T_k^{(j)}$ changes its price $p_{ik}^{(j)}$ for unit bandwidth by Eq. (11), the whole utility of all the path particles in the demand force-field F_D will monotonically decrease in direct proportion to the value of η_2 . When a link particle A_i modifies its allotted bandwidth $a_{ik}^{(j)}$ by Eq. (12), the whole utility of all the link particles in the resource force-field F_R will monotonically decrease in direct proportion to the value of λ_2 .

Theorem 5 For the generalized particle model and algorithm GP, when a path particle $T_k^{(j)}$ changes its price $p_{ik}^{(j)}$ for unit bandwidth by Eq. (11), the potential energy $Q_D(t)$ that is generated by the interactions among the path particles in F_D will monotonically decrease in direct proportion to the value of η_4 . When a link particle A_i modifies its allotted bandwidth $a_{ik}^{(j)}$ by Eq. (12), then the potential energy that is caused by the interactions among the link particles in F_R will monotonically decrease in direct proportion to the value of λ_4 .

Theorem 6 The generalized particle model and algorithm GP can dynamically optimize in parallel the network bandwidth allocation in such a way that the path particle $T_k^{(j)}$ and link particle A_i can dynamically adjust their pricing policy and allocation policy for network bandwidth, their intentional strength for pursuing their own personal utility, and their interactive strength with other path and link particles.

Lemma 2 If $1 - \gamma_1 < \Phi_2(t) < 0$ and $1 - \gamma_2 < \Psi_2(t) < 0$, then the dynamic states of a path particle $T_k^{(j)}$ and link particle A_i will eventually converge to the stable equilibrium states, $v_k^{(j)}(t) \in \{0, 1\}$ and $v_i(t) \in \{0, 1\}$, respectively.

Lemma 3 If $\gamma_1 > 1$, $\Phi_2(t) > 0$ and $\gamma_2 > 1$, $\Psi_2(t) > 0$, then the dynamic states of a path particle $T_k^{(j)}$ and link particle A_i will eventually converge to the stable equilibrium states, $v_k^{(j)}(t) = +1$ and $v_i(t) = +1$, respectively.

Lemma 4 If $\Phi_2(t) < 1 - \gamma_1 < 0$ and $\Psi_2(t) < 1 - \gamma_2 < 0$, then the dynamic states of a path particle $T_k^{(j)}$ and link particle A_i will eventually converge to the stable equilibrium states, $v_k^{(j)}(t) = 0$ and $v_i(t) = 0$, respectively.

Theorem 7 *In the generalized particle model, the dynamic equation (7) and (8) have the stable equilibrium points iff the right side of equation (7) is larger than 0 for $u_i(t) = 1$ and $v_i(t) = 1$; and the right side of equation (8) is larger than 0 for $u_i(t) = 1$ and $v_i(t) = 1$, respectively.*

Theorem 8 *In the generalized particle model, the dynamical Eqs. (7) and (8) have the stable equilibrium points iff there is, respectively:*

$$\gamma_1 > 1 + [\eta_1 + \eta_2 \alpha_1 + \eta_3 \omega_k^{(j)}(t) + \eta_4 \frac{\partial E_D(t)}{\partial u_k^{(j)}(t)}] \sum_{i=1}^m [a_k^{(j)}(t)]^2 / [p_{ik}^{(j)}(t)]^4 \quad (15)$$

$$\gamma_2 > 1 + [\lambda_1 + \lambda_2 \alpha_1 + \lambda_3 \omega_i(t) + \lambda_4 \frac{\partial E_R(t)}{\partial u_i(t)}] \sum_{j=1}^p \sum_{k=1}^{n_j} [p_{ik}^{(j)}(t)]^2 / [a_{ik}^{(j)}(t)]^4 \quad (16)$$

Theorem 9 *If the conditions, (15), (16), remain valid, then the generalized particle model will converge to a stable equilibrium state.*

8 Simulations

We show the application of our GP model and algorithm for the optimal bandwidth assignment to networks. In broadband networks, such as those based on ATM, SDH and SONET, many local network or clients/severs need to be connected via many virtual paths. A virtual path is a semi-persistent connection with certain designated maximal bandwidth and through a cascade of links. Several virtual paths may need the same link and share the bandwidth of the link. Each link has its possible maximal bandwidth. Furthermore, between two nodes that are connected, there could be virtual paths with different bandwidth demands.

Given a set $V = \{(v_i, v_j)\}$ of network node pairs (v_i, v_j) between which communication with bandwidth b_{ij} is requested, each node pair (v_i, v_j) has the corresponding set $T_{ij} = \{T_{ij}^1, \dots, T_{ij}^{k_{ij}}\}$ of possible virtual paths, and each $T_{ij}^k, k \in \{1, \dots, k_{ij}\}$, has a set A_{ij}^k of links where T_{ij}^k passes through. We regard a link with an allowable bandwidth as a network entity; and a virtual path as a network request.

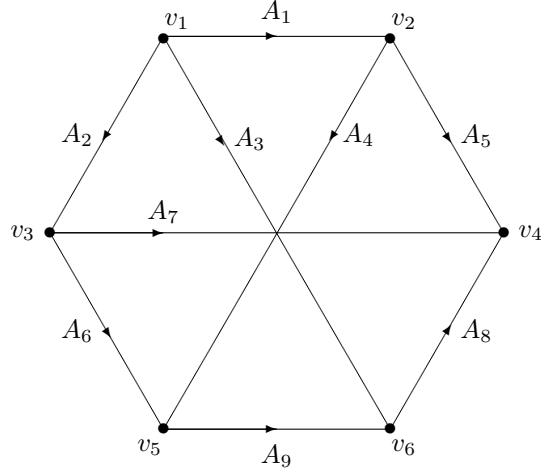


Fig.3 The network topology for bandwidth assignment

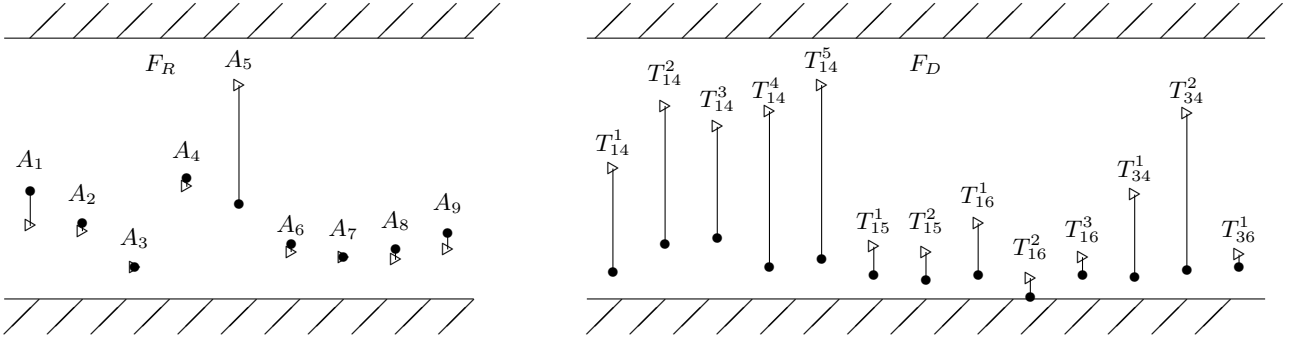


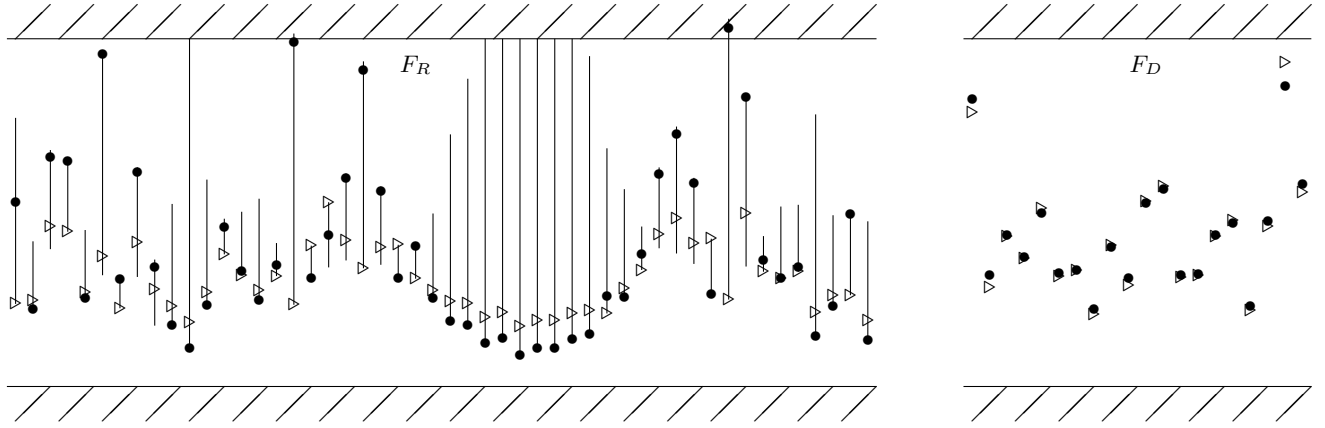
Fig.4 The dynamic process of network bandwidth assignment by using reciprocal dual force-fields (● stable equilibrium positions with pricing policy adjusted by links, ▷ stable equilibrium positions with the fixed pricing policy of links. The vertical real-line: the dynamic range during the transient)

For the network bandwidth assignment shown in Fig.3 the reciprocal dual force-fields model and the algorithm GP are made use of, and the dynamic processes of the simulation are given in Fig.4, where the set of considered node pairs is $V = \{(v_1, v_4), (v_1, v_5), (v_1, v_6), (v_3, v_4), (v_3, v_6)\}$ with the corresponding requested bandwidths: $\{25, 10, 12, 15, 8\}$; the virtual path sets are

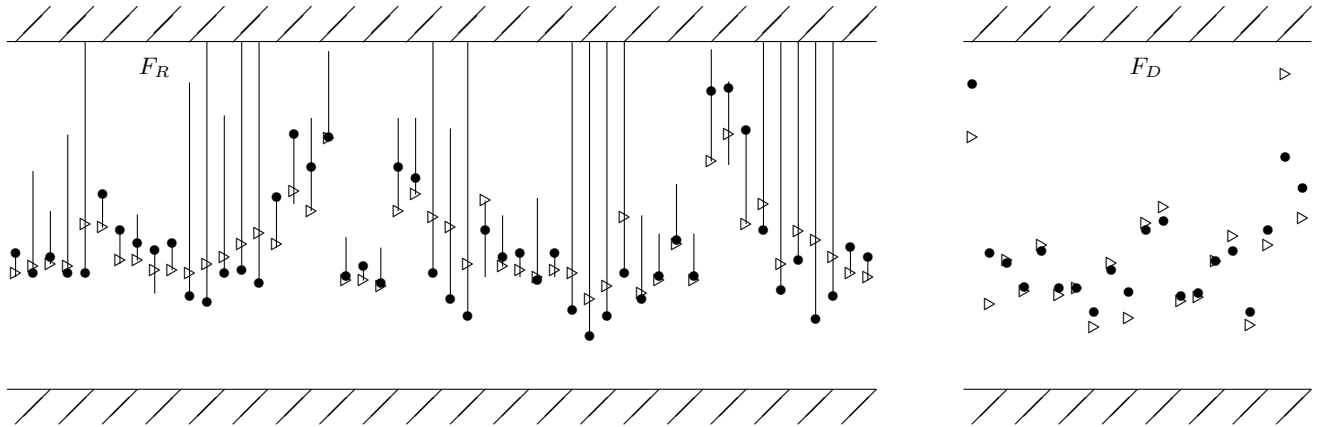
$$\begin{aligned}
T_{14} &= \{T_{14}^1, T_{14}^2, T_{14}^3, T_{14}^4, T_{14}^5\} \\
&= \{(A_1, A_5), (A_3, A_8), (A_2, A_6, A_9, A_8), (A_2, A_7), (A_1, A_4, A_9, A_8)\} \\
T_{15} &= \{T_{15}^1, T_{15}^2\} = \{(A_1, A_4), (A_2, A_6)\} \\
T_{16} &= \{T_{16}^1, T_{16}^2, T_{16}^3\} = \{(A_3), (A_2, A_6, A_9), (A_1, A_4, A_9)\} \\
T_{34} &= \{T_{34}^1, T_{34}^2\} = \{(A_7), (A_6, A_9, A_8)\} \\
T_{36} &= \{T_{36}^1\} = \{(A_6, A_9)\}
\end{aligned}$$

and the set of links is $\{A_1, A_2, A_3, A_4, A_5, A_6, A_7, A_8, A_9\}$

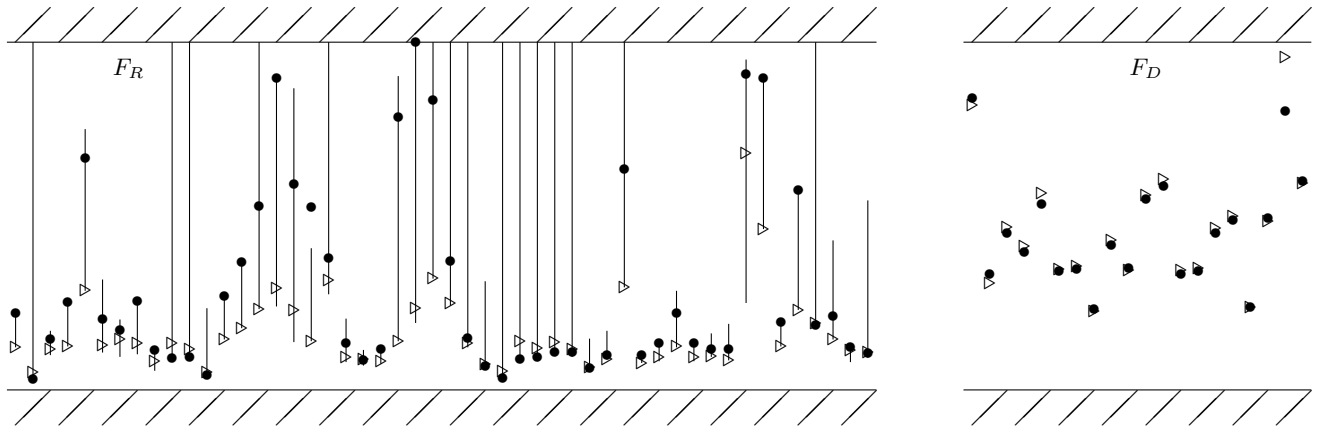
with the allowable maximum bandwidths: $\{10, 15, 30, 16, 20, 18, 20, 27, 25\}$.



(a) The case for balance of supplies and demands



(b) The case for supplies much smaller than demands



(c) The case for supplies much larger than demands

Fig.5 The dynamic process of resource assignment among 50 network entities and 20 network requests (● stable equilibrium positions, with paying policy adjusted by network requests, ▷ stable equilibrium positions with unchangeable paying policy, The vertical real-line: the dynamic range during the transient)

We obtain the solution of bandwidth assignment as follows:

$B_{14} = \{0.9, 13.3, 1.1, 7.2, 2.5\}$ for T_{14} , $B_{15} = \{5.7, 4.3\}$ for T_{15} , $B_{16} = \{11.2, 0, 0.8\}$ for T_{16} , $B_{34} = \{10.4, 4.6\}$ for T_{34} , $B_{36} = \{8.0\}$ for T_{36} .

Next, the network resource assignment for 50 network entities with different resource volumes and 20 network requests with different resource demands is carried out by using the algorithm GP, whose dynamic processes are shown in Fig.5 for three cases: (a) the total resource volumes of all the network entities roughly equal to the volumes required by all the network requests, (b) supplies smaller than demands, and (c) for supplies larger than demands.

9 Conclusions

In this paper, a new generalized particle model and its algorithm for the bandwidth allocation optimization have been proposed, which have powerful processing ability under complex environments that involve the various interactions among network entities, the market mechanism between the demands and service, and other phenomena common in networks, such as congestion, metabolism, and breakdown of network entities. In addition, the generalized particle model algorithm has a practical application prospect because of its low time complexity.

In [12], we take the model in this paper and develop it into a "general" particle model. In that work, we (1) introduce some biases factors to improve the transmission reliability, (2) improve the average satisfaction degree of the users (i.e., paths) and the average utilization of resources (i.e., links) by redefining the interaction potential energy functions, (3) define new hybrid energy functions for the channels and links, and (4) realize that the smaller the utilities of the network entities, the faster the network entities can be optimized. We have applied this extended model to solving the bandwidth allocation problem, and obtained satisfactory results.

Appendix A

Proof of Theorem 1. When allotted bandwidth $a_{ik}^{(j)}$ is updated according to equation (12), the first and the second terms of equation (12) will cause the following speed increments of a link particle, respectively:

$$[du_i(t)/dt]_1 = \sum_{j=1}^p \sum_{k=1}^{n_j} \frac{\partial u_i(t)}{\partial a_{ik}^{(j)}(t)} \frac{da_{ik}^{(j)}(t)}{dt} = -\lambda_1 \sum_{j=1}^p \sum_{k=1}^{n_j} \left[\frac{\partial u_i(t)}{\partial a_{ik}^{(j)}(t)} \right]^2; \quad (13)$$

$$\begin{aligned} [du_i(t)/dt]_2 &= \sum_{j=1}^p \sum_{k=1}^{n_j} \frac{\partial u_i(t)}{\partial a_{ik}^{(j)}(t)} \frac{da_{ik}^{(j)}(t)}{dt} = -\lambda_2 \sum_{j=1}^p \sum_{k=1}^{n_j} \frac{\partial u_i(t)}{\partial a_{ik}^{(j)}(t)} \frac{\partial J_R(t)}{\partial a_{ik}^{(j)}(t)} \\ &= -\lambda_2 \sum_{j=1}^p \sum_{k=1}^{n_j} \frac{\partial u_i(t)}{\partial a_{ik}^{(j)}(t)} \frac{\partial J_R(t)}{\partial u_i(t)} \frac{\partial u_i(t)}{\partial a_{ik}^{(j)}(t)} = -\lambda_2 \sum_{j=1}^p \sum_{k=1}^{n_j} \frac{\partial J_R(t)}{\partial u_i(t)} \left[\frac{\partial u_i(t)}{\partial a_{ik}^{(j)}(t)} \right]^2. \end{aligned} \quad (14)$$

Similarly, the third and fourth terms of equation (12) will cause the following speed increments of a link particle, respectively, which are related to $P_R(t)$ and $Q_R(t)$.

$$[du_i(t)/dt]_3 = -\lambda_3 \sum_{j=1}^p \sum_{k=1}^{n_j} \frac{\partial P_R(t)}{\partial u_i(t)} \left[\frac{\partial u_i(t)}{\partial a_{ik}^{(j)}(t)} \right]^2; \quad [du_i(t)/dt]_4 = -\lambda_4 \sum_{j=1}^p \sum_{k=1}^{n_j} \frac{\partial Q_R(t)}{\partial u_i(t)} \left[\frac{\partial u_i(t)}{\partial a_{ik}^{(j)}(t)} \right]^2.$$

Therefore, if the allotted bandwidth $a_{ik}^{(j)}$ is updated according to equation (12), then the speed increment of the link particle A_i will become $\Psi_2(t)$ of Eq. (8), namely

$$\sum_{k=1}^4 [du_i(t)/dt]_k = -\left[\lambda_1 + \lambda_2 \frac{\partial J_R(t)}{\partial u_i(t)} + \lambda_3 \frac{\partial P_R(t)}{\partial u_i(t)} + \lambda_4 \frac{\partial Q_R(t)}{\partial u_i(t)} \right] \sum_{j=1}^p \sum_{k=1}^{n_j} \left[\frac{\partial u_i(t)}{\partial a_{ik}^{(j)}(t)} \right]^2 = \Psi_2(t).$$

Similarly, it follows that, if the unit bandwidth price $p_{ik}^{(j)}$ is updated by Eq. (11), the speed increment of the path particle $T_k^{(j)}$ will be equal to $\Phi_2(t)$ of Eq. (7).

Proof of Theorem 2. According to Eqs. (13), (14), the sum of the first and second terms of Eq. (12) will be

$$\begin{aligned} [du_i(t)/dt]_{1+2} &= [du_i(t)/dt]_1 + [du_i(t)/dt]_2 = -\lambda_1 \sum_{j=1}^p \sum_{k=1}^{n_j} \left[\frac{\partial u_i(t)}{\partial a_{ik}^{(j)}(t)} \right]^2 - \lambda_2 \sum_{j=1}^p \sum_{k=1}^{n_j} \frac{\partial J_R(t)}{\partial u_i(t)} \left[\frac{\partial u_i(t)}{\partial a_{ik}^{(j)}(t)} \right]^2 \\ &= -(\lambda_1 + \alpha_2 \lambda_2) \sum_{j=1}^p \sum_{k=1}^{n_j} [p_{ik}^{(j)}(t) u_i(t)]^2 / [a_{ik}^{(j)}(t)]^4 \leq 0. \end{aligned}$$

Similarly, the sum of the first and second terms of Eq. (11) will be

$$\begin{aligned} [du_k^{(j)}(t)/dt]_{1+2} &= -\eta_1 \sum_{i=1}^m \left[\frac{\partial u_k^{(j)}(t)}{\partial p_{ik}^{(j)}(t)} \right]^2 + -\eta_2 \sum_{i=1}^m \frac{\partial J_D(t)}{\partial u_k^{(j)}(t)} \left[\frac{\partial u_k^{(j)}(t)}{\partial p_{ik}^{(j)}(t)} \right]^2 \\ &= -(\eta_1 + \alpha_1 \eta_2) \sum_{i=1}^m [a_{ik}^{(j)}(t) u_i(t)]^2 / [p_{ik}^{(j)}(t)]^4 \leq 0. \end{aligned}$$

Proof of Lemma 1. For F_R , supposing that $H(t) = \max_i [u_i(t)]^2$, we have

$$[\exp(H(t)/2\epsilon^2)]^{2\epsilon^2} \leq [\sum_{i=1}^m \exp(u_i(t)/2\epsilon^2)]^{2\epsilon^2} \leq [m \exp(H(t)/2\epsilon^2)]^{2\epsilon^2},$$

Simultaneously taking the logarithm of both sides of the above inequalities will lead to

$$H(t) \leq 2\epsilon^2 \ln \sum_{i=1}^m \exp(H(t)/2\epsilon^2) \leq H(t) + 2\epsilon^2 \ln m,$$

Since m is constant and ϵ is very small, we have

$$H(t) \approx 2\epsilon^2 \ln \sum_{i=1}^m \exp(H(t)/2\epsilon^2) - 2\epsilon^2 \ln m = 2P_R(t).$$

It turns out that the potential energy $P_R(t)$ at the time t represents the maximum of $u_i(t)$ among all the link particles A_i , $i \in \{1, \dots, m\}$; namely, the minimum of the personal utilities among A_i at time t . Hence the decrease of the potential energy $P_R(t)$ will result in the increase of the utility of such a link whose utility is the minimal among all links. Similarly, it follows that the decrease of the potential energy $P_D(t)$ will result in the increase of the utility of such a path whose utility is the minimal among all the paths.

Proof of Theorem 3. When a link particle A_i changes the allotted bandwidth $a_{ik}^{(j)}$ according to Eq. (12), the differentiation of the potential energy function $P_R(t)$ with respect to time is denoted by $[\frac{dP_R(t)}{dt}]$. By Theorem 1, the speed increment of link particle A_i , that is related to potential energy $P_R(t)$, is given by

$$[du_i(t)/dt]_3 = -\lambda_3 \sum_{j=1}^p \sum_{k=1}^{n_j} \frac{\partial P_R(t)}{\partial u_i(t)} \left[\frac{\partial u_i(t)}{\partial a_{ik}^{(j)}} \right]^2.$$

We thus have

$$\begin{aligned} \left[\frac{dP_R(t)}{dt} \right] &= \frac{\partial P_R(t)}{\partial u_i(t)} \left[\frac{du_i(t)}{dt} \right]_3 = -\lambda_3 \sum_{j=1}^p \sum_{k=1}^{n_j} \left[\frac{\partial P_R(t)}{\partial u_i(t)} \right]^2 \left[\frac{\partial u_i(t)}{\partial a_{ik}^{(j)}} \right]^2 \\ &= -\lambda_3 \omega_i^2(t) u_i^4(t) \sum_{j=1}^p \sum_{k=1}^{n_j} [p_{ik}^{(j)}(t)]^2 / [a_{ik}^{(j)}(t)]^4 \leq 0. \end{aligned}$$

It turns out that, when the allotted bandwidth $a_{ik}^{(j)}$ is updated by using Eq. (12), $P_R(t)$ will monotonically decrease. Then by Lemma 1, the decrease of $P_R(t)$ will result in the increase of the minimal utility among all the link particles in direct proportion to the value of $\lambda_3 \omega_i^2(t)$.

Similarly, it follows that, when price $p_{ik}^{(j)}$ for unit bandwidth is updated by Eq. (11), the minimal utility of all the path particles will monotonically increase in direct proportion to the value of $\eta_3 [\omega_k^{(j)}(t)]^2$.

Proof of Theorem 4. Similar to the proof of Theorem 1, it follows that, when a link particle A_i modifies its allotted bandwidth $a_{ik}^{(j)}$ by Eq. (12), then differentiation of $J_R(t)$ with respect to time t will be negative, i.e. $\lceil \frac{dJ_R(t)}{dt} \rceil \leq 0$, and it is directly proportional to the value of λ_2 . Similarly, we can see that $\lceil \frac{dJ_D(t)}{dt} \rceil \leq 0$ and it is directly proportional to the value of η_2 .

Proof of Theorem 5. Similar to Theorem 1, we can get $\lceil \frac{dQ_D(t)}{dt} \rceil \leq 0$, $\lceil \frac{dQ_R(t)}{dt} \rceil \leq 0$, which are directly proportional to η_4 and λ_4 , respectively.

Proof of Theorem 6. By Theorem 1 through Theorem 5, it is straightforward. In summary, $(\eta_1 + \alpha_1 \eta_2)$ and $(\lambda_1 + \alpha_2 \lambda_2)$ represent the intentional strength for a path particle $T_k^{(j)}$ and link particle A_i to pursue their own personal utility, respectively; η_2 and λ_2 represent the intentional strength for them to take into account the whole utility of all the path particles and link particles, respectively; $\eta_3 [\omega_k^{(j)}(t)]^2$ and $\lambda_3 \omega_i^2(t)$ represent the intentional strength for them to increase the minimal personal utility among all the path particles and link particles, respectively. η_4 and λ_4 represent the interactive strength for them to interact with other path particles and link particles, respectively.

Proof of Lemma 2. For $\gamma_2(t) > 1$, the $\Psi_1(t)$ of a link particle A_i is a piecewise linear function of the stimulus $u_i(t)$, as shown by three segments: Segment I, Segment II, and Segment III in Fig.6. By Eq. (8), $du_i(t)/dt = 0$ holds true iff $-\Psi_2(t) = \Psi_1(t)$, which means that an intersection point between $-\Psi_2(t)$ and $\Psi_1(t)$ as the functions of $u_i(t)$ in Fig.6 is an equilibrium point. We see that, for the case of $1 - \gamma_2 < \Psi_2(t) < 0$, there are three intersection points between $-\Psi_2(t)$ and $\Psi_1(t)$, among which only the intersection points on the Segment I and Segment III, e.g. p_3 and p_4 , are stable, that correspond to $v_i(t) = 0$, $u_i(t) < 0$ and $v_i(t) = 1$, $u_i(t) > 1$, respectively. The proof for a path particle $T_k^{(j)}$ is similar.

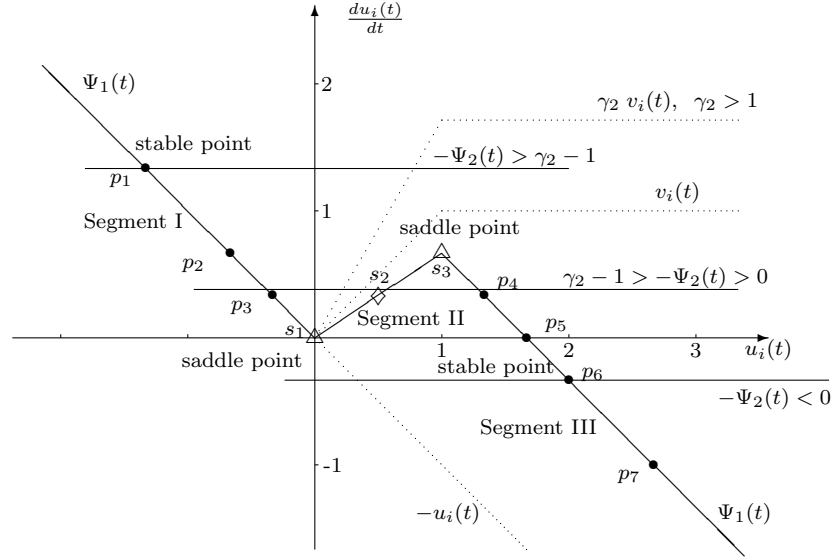


Fig.6 When $\gamma_2 > 1$, the reachable equilibrium points of the dynamic status $v_i(t)$ of a link particle A_i . The point where $\Psi_2(t)$ equals $\Psi_1(t)$ is an equilibrium point. \bullet , \triangle and \diamond denote a stable equilibrium point, saddle point and unstable equilibrium point, respectively.

Proof of Lemma 3. If $\gamma_2(t) > 1$ and $\Psi_2(t) > 0$, then the intersection points between $-\Psi_2(t)$ and $\Psi_1(t)$ of a link particle A_i are all located on Segment III, e.g. p_6 . Therefore A_i has the stable equilibrium points with $v_i(t) = 1$, $u_i(t) > 1$. The proof for a path particle $T_k^{(j)}$ is similar.

Proof of Lemma 4. If $\Psi_2(t) < 1 - \gamma_2 < 0$, then $-\Psi_2(t)$ and $\Psi_1(t)$ of a link particle A_i only has the intersection points on Segment I, e.g. p_1 . Therefore A_i has the stable equilibrium points with $v_i(t) = 0$, $u_i(t) < 0$. The proof for a path particle $T_k^{(j)}$ is similar.

Proof of Theorem 7. By Eqs. (1), (2), we have $u_k^{(j)}(t) \geq 0$ and $u_i(t) \geq 0$. Thereby, we only consider the equilibrium points with $u_k^{(j)}(t) \geq 0$ and $u_i(t) \geq 0$. The right side of Eq. (8) is denoted by RHS.

Sufficiency. Assume that, for Eq. (8), $RHS > 0$ holds for $u_i(t) = 1$, $v_i(t) = 1$. It follows that $-\Psi_2(t) \neq \Psi_1(t)$ for $u_i(t) = 1$, $v_i(t) = 1$, namely, it is impossible that the equilibrium point is the intersection point s_3 between Segment II and Segment III. Note that the saddle point s_3 isn't stable equilibrium point. Thus $RHS = \frac{du_{ij}(t)}{dt} > 0$ leads to the stable equilibrium points of A_i on Segment III.

Necessity. Suppose that Eq. (8) has a stable equilibrium point. we need to prove that $RHS > 0$ holds for $u_k^{(j)}(t) = 1$ and $v_k^{(j)}(t) = 1$. By contrary, if there is $RHS \leq 0$, then the equilibrium point must be

either at the point s_3 for the case of $RHS = 0$, or on Segment II for the case of $RHS < 0$. Since the point s_3 and the points on Segment II are all not stable, a contradiction happens.

Similarly, we can prove for Eq. (7).

Proof of Theorem 8. By Eqs. (1), (3), (5), (7), we have

$$\Phi_2(t) = -[\eta_1 + \eta_2 \alpha_1 + \eta_3 \omega_k^{(j)}(t) u_k^{(j)}(t) + \eta_4 \frac{\partial E_D(t)}{\partial u_k^{(j)}(t)}] [u_k^{(j)}(t)]^2 \sum_{i=1}^m [a_k^{(j)}(t)]^2 / [p_{ik}^{(j)}(t)]^4.$$

According to Theorem (7), the dynamic equation (7) has a stable equilibrium point iff

$$\gamma_1 - 1 - [\eta_1 + \eta_2 \alpha_1 + \eta_3 \omega_k^{(j)}(t) + \eta_4 \frac{\partial E_D(t)}{\partial u_k^{(j)}(t)}] \sum_{i=1}^m [a_k^{(j)}(t)]^2 / [p_{ik}^{(j)}(t)]^4 > 0.$$

Similarly, by Eqs. (2), (4), (6), (8), we have

$$\Psi_2(t) = -[\lambda_1 + \lambda_2 \alpha_1 + \lambda_3 \omega_i(t) u_i(t) + \lambda_4 \frac{\partial E_R(t)}{\partial u_i(t)}] [u_i(t)]^2 \sum_{j=1}^p \sum_{k=1}^{n_j} [p_{ik}^{(j)}(t)]^2 / [a_{ik}^{(j)}(t)]^4.$$

According to Theorem (7), the dynamic equation (8) has a stable equilibrium point iff

$$\gamma_2 - 1 - [\lambda_1 + \lambda_2 \alpha_1 + \lambda_3 \omega_i(t) + \lambda_4 \frac{\partial E_R(t)}{\partial u_i(t)}] \sum_{j=1}^p \sum_{k=1}^{n_j} [p_{ik}^{(j)}(t)]^2 / [a_{ik}^{(j)}(t)]^4 > 0.$$

Proof of Theorem 9. For the force-field F_R , we define a Lyapunov function $L_R(t)$ by

$$\begin{aligned} L_R(t) = & -\frac{1}{2} \sum_i^m (\gamma_2 - 1) v_i(t)^2 + \sum_i^m \int_0^t \frac{dv_i(\tau)}{d\tau} [\lambda_1 + \lambda_2 \alpha_1 + \lambda_3 \omega_i(\tau) u_i(\tau) \\ & + \lambda_4 \frac{\partial E_R(\tau)}{\partial u_i(\tau)}] [u_i(\tau)]^2 \sum_{j=1}^p \sum_{k=1}^{n_j} [p_{ik}^{(j)}(\tau)]^2 / [a_{ik}^{(j)}(\tau)]^4 d\tau, \end{aligned}$$

We hence have

$$\begin{aligned} |L_R(t)| \leq & \sum_i^m (\gamma_2 - 1) |v_i(t)|^2 + \sum_i^m \int_0^t \left| \frac{dv_i(\tau)}{d\tau} \right| \cdot |[\lambda_1 + \lambda_2 \alpha_1 + \lambda_3 \omega_i(\tau) u_i(\tau) \\ & + \lambda_4 \frac{\partial E_R(\tau)}{\partial u_i(\tau)}]| \cdot [u_i(\tau)]^2 \sum_{j=1}^p \sum_{k=1}^{n_j} [p_{ik}^{(j)}(\tau)]^2 / [a_{ik}^{(j)}(\tau)]^4 d\tau. \end{aligned}$$

Since the condition (16) is valid, $v_i(t) \leq 1$ by Eq. (10) in Definition 4, and $u_i(t) \leq \varsigma_2$ by Eq. (2) in Definition 1, it follows that

$$|L_R(t)| \leq \sum_i^m (\gamma_2 - 1) + \varsigma_1^2 \sum_i^m \gamma_2 < m\gamma_2 (\varsigma_1^2 + 1).$$

which implies that $L_R(t)$ is bounded.

In addition, we have

$$\frac{dL_R(t)}{dt} = - \sum_i^m (\gamma_2 - 1) v_i(t) \frac{dv_i(t)}{dt} + \sum_i^m \frac{dv_i(t)}{dt} [\lambda_1 + \lambda_2 \alpha_1 + \lambda_3 \omega_i(t) u_i(t)$$

$$\begin{aligned}
& +\lambda_4 \frac{\partial E_R(t)}{\partial u_i(t)}] (u_i(t))^2 \sum_{j=1}^p \sum_{k=1}^{n_j} (p_{ik}^{(j)}(t))^2 / (a_{ik}^{(j)}(t))^4 \\
= & -\sum_i^m \frac{dv_i(t)}{du_i(t)} \frac{du_i(t)}{dt} \{ -u_i(t) + \gamma_2 v_i(t) - [\lambda_1 + \lambda_2 \alpha_1 + \lambda_3 \omega_i(t) u_i(t) \\
& +\lambda_4 \frac{\partial E_R(t)}{\partial u_i(t)}] (u_i(t))^2 \sum_{j=1}^p \sum_{k=1}^{n_j} (p_{ik}^{(j)}(t))^2 / (a_{ik}^{(j)}(t))^4 \} \\
= & -\sum_i^m \frac{dv_i(t)}{du_i(t)} \left(\frac{du_i(t)}{dt} \right)^2.
\end{aligned}$$

Note that

$$\frac{dv_i(t)}{du_i(t)} = \begin{cases} 1 & \text{if } 0 < u_i(t) < 1; \\ 0 & \text{otherwise;} \end{cases}$$

Thereby, we have

$$\frac{dL_R(t)}{dt} \leq 0,$$

that is, $L_R(t)$ will decrease monotonically as time elapses.

Similarly, we can define a Lyapunov function $L_D(t)$ for the force-field F_D , and then prove that it is bounded and monotonically decrease with time.

References

- [1] Kelly, F. P.. Charging and Rate Control for Elastic Traffic. European Transactions on Telecommunications, 1997, 29: 1009-1016.
- [2] Kelly, F.P., A. Maulloo and D. Tan. Rate Control in Communication Networks: Shadow Prices, Proportional Fairness and Stability. Journal of the Operational Research Society, 1998, 49: 237-252.
- [3] Kelly, F.P.. Mathematical Modeling of the Internet, in B. Engquist and W. Schmid (ed.). Mathematics Unlimited - 2001 and Beyond, Springer-Verlag, Berlin, 2001, 685-702.
- [4] S.H. Low. A duality model of TCP and Queue management algorithms. IEEE ACM Transactions on Networking, 2003, 11(4): 525-536.
- [5] S.H. Low, F. Paganini, L. Wang, J.C. Doyle. Linear stability of TCP/RED and a scalable control. Computer Networks 43 (2003) 633-647.
- [6] S.H. Low, F. Paganini, J.C. Doyle. Internet congestion control. IEEE Control Systems Magazine, 2002, 22(2): 28-43.
- [7] S.H. Low, L. Peterson, L. Wang. Understanding vegas: a duality model. Journal of ACM, 2002, 49(2): 207-235.
- [8] Marco Dorigoa, Christian Blumb. Ant colony optimization theory: A survey. Theoretical Computer Science. 2005, 344: 243-278.
- [9] Son Hong Ngo, Xiaohong Jiang, Susumu Horiguchi. An ant-based approach for dynamic RWA in opticalWDM networks. Photonic Network Communications, 2006, 11: 39-48.
- [10] D. Bertsekas and R. Gallager. Data Networks. Prentice-Hall, New Jersey, 1992.
- [11] D.X. Shuai, X. Feng. Distributed Problem Solving in Multi-Agent Systems: A Spring Net Approach. IEEE Intelligent Systems. 2005, 20(4): 66-74.
- [12] D. X. Shuai, X. Feng. The parallel optimization of network bandwidth allocation based on generalized particle model, Computer Networks 50 (9) (2006) 1219-1246.